RSC Advances

PAPER

View Article Online
View Journal | View Issue

Cite this: *RSC Adv.*, 2020, **10**, 18025

Facile control of surfactant lamellar phase transition and adsorption behavior†

Rui A. Gonçalves,[a] Polina Naidjonoka,[b] Tommy Nylander,[b] Maria G. Miguel,[c] Björn Lindman[ab] and Yeng Ming Lam *[a]

This study sets out to investigate the effect of the presence of small water-soluble additives on the tunability of the surfactant gel-to-liquid crystalline (L_β–L_α) phase transition temperature (T_m) for a bilayer-forming cationic surfactant and the phase behavior of such surfactant systems on dilution. This is strongly driven by the fact that this type of cationic surfactant has many interesting unanswered scientific questions and has found applications in various areas such as consumer care, the petrochemical industry, food science, *etc.* The underlying surfactant/additive interactions and the interfacial behavior of lamellar surfactant systems including the surfactant deposition on surfaces can provide new avenues to develop novel product formulations. We have examined dioctadecyldimethyl ammonium chloride (DODAC) in the presence of small polar additives, with respect to the phase behavior upon dilution and the deposition on silica. Differential scanning calorimetry (DSC) is used to track the transition temperature, T_m, and synchrotron and laboratory-based small and wide-angle X-ray scattering (SAXS and WAXS) were used to determine the self-assembled surfactant structure below and above the T_m. DSC scans showed that upon dilution the additives could be removed from the surfactant bilayer which in turn tuned the T_m. A spontaneous transition from a liquid crystalline (L_α) phase to a gel (L_β) phase on dilution was demonstrated, which indicated that additives could be taken out from the L_α phase. By means of *in situ* null ellipsometry, the deposition of a diluted surfactant L_β phase upon replacement of bulk solution by deionized water was followed. This technique enables time-resolved monitoring of the deposited surfactant layer thickness and adsorbed amount, which allows us to understand the deposition on surfaces. Robust layers at least one bilayer-thick were deposited onto the surface and shown to be irreversibly adsorbed due to poor surfactant solvency in water. The thickest layer of surfactant deposited after dilution was found for mixtures with small amounts of additive since high amounts might lead to a phase-separated system.

Received 12th February 2020
Accepted 8th April 2020

DOI: 10.1039/d0ra01340d

rsc.li/rsc-advances

1. Introduction

The function of materials is often determined by their surface properties, *i.e.* where the material meets the surrounding medium. Deposition of a functional layer on a surface is, therefore, crucial for controlling material properties such as lubrication and protection against contamination. It is challenging to prepare molecularly thin layers, and in particular, with controlled thickness and surface properties for such studies. Amphiphilic molecules, such as surfactants and lipids, can adsorb from aqueous solution and deposit on hydrophobic and hydrophilic surfaces forming monomolecularly thin layers. Such layers are, however, not very stable when exposed to water or humid air since they are made from substances with a significant solubility in water. Stable layers can either be obtained by chemically coupling the molecules onto the surface or between the adsorbed molecules. One example where the former concept is used is in the case where molecules with thiol end groups are used to modify gold surfaces and this has led to the development of some important practical applications.[1–3]

Another principle for the preparation of monomolecular layers is built on spreading insoluble amphiphilic compounds on the air–water interface. This monolayer can be transferred to solid surface passing through the interface. Multilayers can be obtained in this way by letting the solid surface pass through the water–air interface several times. This is the basis for the well-established Langmuir–Blodgett method.[4]

In hair conditioning the general principle is to render hair with net positive charges, creating an electrostatic repulsion. This can be achieved by either cationic surfactants or cationic polymers and both principles have been used successfully and

[a]*School of Materials Science and Engineering, Nanyang Technological University, 639798 Singapore, Singapore. E-mail: YMLam@ntu.edu.sg*

[b]*Division of Physical Chemistry, Department of Chemistry, Centre for Chemistry and Chemical Engineering, Lund University, SE-221 00 Lund, Sweden*

[c]*Department of Chemistry, University of Coimbra, 3004-535 Coimbra, Portugal*

† Electronic supplementary information (ESI) available. See DOI: 10.1039/d0ra01340d

are common in commercial hair conditioners. For the creation of robust layers in a simple procedure, however, alternatives to the indicated general principles have to be found.

The adsorption of soluble, low molecular weight substances is typically reversible, however polymers often display a more or less irreversible adsorption, especially for high molecular weight polymers. Charged polymers have a higher solubility in water and adsorb mainly when the surface is oppositely charged.[5,6] This adsorption is effectively irreversible for higher molecular weight polymers. Polyelectrolyte adsorption has been thoroughly studied during recent decades and is exploited in many applications. For example, it is possible to charge up surfaces through adsorption and by using the irreversibility of adsorption also reverse the charge of a surface. A practical application of charging up surfaces is in conditioning ("two-in-one") hair shampoo where a cationic polymer is deposited on hair from a mixed solution of an anionic surfactant and a cationic polymer. With an excess of surfactant, such a formulation is thermodynamically stable, and no adsorption onto hair occurs. However, on rinsing with water, the system falls into the two-phase region of the phase diagram and deposition occurs; further rinsing leads to removal of the surfactant whereas the polymer remains and this gives the substrate the desired positive charge and a conditioning effect. The mechanism is well understood from phase diagrams, and the deposition has been demonstrated in *in situ* adsorption studies using ellipsometry.[7–12]

Alternatively, surfactants can be used for hair conditioning. Normally cationic surfactants or different mixed systems are used.[13] A good conditioning effect normally is based on achieving a layer of cationic surfactant in the lamellar gel (normally referred to as L_β) state. Here the surfactant molecules are in a solid-like state whereby robust layers are formed, and desorption is slow because of very low solubility. Often cationic surfactants with two long alkyl chains are used. Problems with such formulations include the limited kinetic stability of the formulations and the difficulty in controlling the thickness of the deposited layers. In our previous work, we demonstrated the ability to tune the main phase transition temperature by using additives which are preferably located at the surfactant–water interface.[14] Small polar molecules are known to be active in affecting the bilayer fluidity in biological systems. These systems also comprise double-chained amphiphiles, and the mechanisms will be the same for biological systems and surfactant systems.[15–17] Also, hydrotrope molecules have been used in the formulation of personal care products, which make them favorable candidates to tune the phase behavior of surfactant mixtures.

The purpose of the present study was to reveal whether a well-defined layer of surfactant in the L_β state could be achieved by a controlled phase transition from a stable surfactant phase, in particular, a lamellar liquid crystalline phase (L_α). For this purpose, we investigate whether addition of water-soluble components acting as co-surfactants can induce the required phase transition. Furthermore, *in situ* null ellipsometry studies were performed to determine the amount of surfactant deposited and the adsorbed layer thickness. We here show that ternary surfactant–additive–water mixtures in the lamellar liquid crystalline state can be designed in such a way that they are converted into the lamellar gel phase in excess of water. These are then deposited on surfaces in thin layers of well-defined thickness.

2. Experimental

2.1. Materials and sample preparation

Dioctadecyldimethylammonium chloride (DODAC, 96.7% purity) was supplied by Evonik Corporation, USA. Acetic acid, propionic acid and butyric acid were purchased from Sigma-Aldrich, Singapore. Benzyl alcohol was supplied by Ineos Chlorotoluenes, Belgium, and phenoxyethanol supplied by Clariant Produkte GmbH, Germany. These compounds (Scheme 1) were used as received. Ultrapure water of 18 mΩ conductivity was used to prepare the samples (described as original samples). Binary DODAC–water and ternary DODAC–water–additive mixtures were prepared as described previously.[14] Diluted samples were prepared by weighting a fraction of the original sample and diluting in a 1 : 10 sample/water ratio, on a screw-cap glass vial. All the samples were equilibrated at room temperature for, at least, seven days before characterization.

2.2. Differential scanning calorimetry

A discovery DSC differential scanning calorimeter (TA Instruments, USA) was used to determine the main phase transition temperature (T_m) under a heating/cooling cycle at of 2 °C min^{-1} from 10 to 60 °C, and back to 10 °C. The chamber was kept under a nitrogen environment. The software Trios (TA Instruments, USA) was used to calculate the enthalpy associated with the phase transition (ΔH_m).

2.3. Small and wide-angle X-ray scattering

SAXS and WAXS characterization was carried out using two X-ray source instruments. A simultaneous SAXS/WAXS laboratory instrument, Nano-inXider (Xenocs), equipped with a micro-focus source generating X-rays of a wavelength $\lambda = 1.542$ Å (Genix3D) operating at 50 kV and 0.6 mA was used to characterize the original mixtures. The small and wide-angle X-ray scattering beamline at the Australian Synchrotron operating with incident X-rays beam of a wavelength $\lambda = 1.512$ Å (8.2 keV beam) with a Pilatus 2M detector located at 7000 mm was used

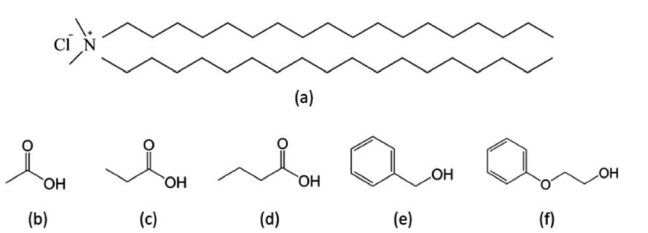

Scheme 1 Molecular structures of: (a) dioctadecyldimethylammonium chloride – DODAC, (b) acetic acid – AA, (c) propionic acid – PA, (d) butyric acid – BA, (e) benzyl alcohol – BenOH, and (f) phenoxyethanol – PhEtOH.

for SAXS. An incident X-rays beam of a wavelength $\lambda = 0.827$ Å (15 keV beam) with a Pilatus 2M detector located at 320 mm was used for WAXS. Fluid samples were loaded into thin-walled borosilicate capillaries (1.5 mm outer diameter, 0.01 mm wall thickness, Hampton Research) and mounted to a multi-capillary block connected to a water bath for thermal behavior studies. The system was calibrated using a AgBeh standard. Each sample was exposed to the beam for 600 seconds using the Nano-inXider, and 1 second at the synchrotron. The combination of SAXS and WAXS profiles allowed to characterize the surfactant mixtures. The resulting 2D scattering profiles were integrated to 1D background-corrected profiles using Foxtrot software (Xenocs) and ScatterBrain software (Australian Synchrotron).

2.4. Surfactant adsorption on surfaces

2.4.1. *In situ* null ellipsometry. The layer thickness and the adsorbed amount of the deposited layers were measured using an automated Rudolph Research thin-film null ellipsometer type 43603-200E. The measurements were conducted using a xenon arc lamp with a filter at a wavelength of 4015 Å.

The optical characteristics of silicon wafer, *i.e.* the refractive index of silicon as well as the thickness and refractive index of the silicon oxide layer, were determined in air and in deionized water as explained in detail by Tiberg and Landgren.[18] In order to correct imperfections of the optical components, four-zone measurements at the beginning of each experiment were used.

The adsorption from additive/surfactant mixtures was initiated by injecting 0.5 mL of the stock solution into the trapezoid cuvette filled with 4.5 mL of deionized water. The solution in the cuvette was agitated with a magnetic bid rotating at about 300 rpm. The adsorption process was followed by recording the ellipsometric angles for approximately 3500 s, when steady-state was reached. The experiments were conducted at 25 °C ± 0.1 °C by circulating water from a thermostat bath through the cuvette holder. In the rinse experiments, the bulk solution initially in the cuvette was exchanged by flowing deionized water through the measurement cell by means of a peristaltic pump under a flow rate of 10 mL min^{-1}.

The ellipsometer is used to measure the relative change in amplitude, Ψ, and phase shift, Δ, upon reflection of polarized light against a surface. In order to convert Ψ and Δ into layer thickness and refractive index, a four-layer optical model assuming an isotropic medium and planar surface was applied.[19] From the obtained values of the thickness and refractive index, the adsorbed amount, Γ, was calculated using de Feijter's formula:[20]

$$\Gamma = d_f(n_f - n_0)/(dn/dc)$$

where Γ is the mass per surface area (mg m^{-2}), d_f is the thickness of the adsorbed layer (Å), n_f is the refractive index of the adsorbed film, n_0 is the refractive index of the bulk solution, and dn/dc is the refractive index increment. A dn/dc value in the range 0.16–0.18 cm^3 g^{-1} has been used for phospholipid systems.[21,22] In this study we used a dn/dc value of 0.18 cm^3 g^{-1} which gives amounts consistent with results from X-ray characterization of DODAC bilayers previously reported.[14]

2.4.2. Hydrophilic silica surface. The surface used in this study was prepared from silicon wafer, p-type, boron-doped, resistivity 1–20 Ω cm, purchased from SWI (Semiconductor Wafer, Inc., Taiwan). This substrate was thermally oxidized at *ca.* 900 °C to yield a 300 Å-thick layer of silicon oxide in order to increase the resolution of the ellipsometry measurements. The silicon wafer was cut into 12 × 20 mm slices. The silicon substrates were cleaned in a boiling mixture (1 : 1 : 5 by volume) of 25% NH_4OH (pro analysis, Merck), 30% H_2O_2 (pro analysis, Merck) and H_2O at 80 °C for 5 min, followed by cleaning in a boiling mixture (1 : 1 : 5 by volume) of 32% HCl (pro analysis, Merck), 30% H_2O_2 (pro analysis, Merck) and H_2O at 80 °C for 5 min. Then the slides were thoroughly rinsed with deionized water and ethanol and stored in absolute ethanol until use. Before use in the ellipsometry measurement, the substrate was dried with nitrogen and treated in a plasma cleaner (Harrick Scientific Corp., model PDC-3XG) for 5 min in air plasma at 0.02 mbar.

3. Results and discussion

3.1. Effects of the presence of an additive on the T_m

The gel-to-liquid crystalline (L_β–L_α) phase transition temperature (T_m) and the enthalpy of phase transition (ΔH_m) of the surfactant mixtures were determined by differential scanning calorimetry (DSC). The corresponding surfactant chain packing was determined by small and wide-angle X-ray scattering and will be discussed in the next section.

Fig. 1 shows the DSC heating thermograms of the ternary surfactant–additive–water mixtures. Here we present the effect of three short-chain fatty acids (SCFAs): acetic, propionic and butyric acid; and two hydrotrope molecules: benzyl alcohol and phenoxyethanol on the thermal behavior of dioctadecyldimethylammonium chloride (DODAC) in water. The full lines represent the original samples without additive and with 5 (blue color) and 12.5 wt% (orange color) of additive, and the dotted lines correspond to the samples diluted with water. Only one thermal transition was detected for all the mixtures within the investigated temperature range (10 to 60 °C), for both the original sample as well as the same sample after dilution ten times with water. This suggests that with the dilution of the mixtures using water, the same types of self-assembled structures were maintained below and above the T_m, *i.e.* with the lamellar arrangement. The original and diluted samples therefore appear to be in a gel (L_β) phase below the T_m, and in the liquid crystalline (L_α) phase above the respective T_m. The original samples with additive show a lowered T_m but on dilution with water a shift of the T_m to a higher temperature was observed for all the samples. For instance, Fig. 1(b) displays the thermal behavior of the DODAC in the presence of small amount (5 wt%) of acetic acid. A T_m of around 43.5 and 45.5 °C was found for the original sample and the diluted sample, respectively.

The shape of the endothermic peaks is similar for all the mixtures. This suggests that all additives affect the phase

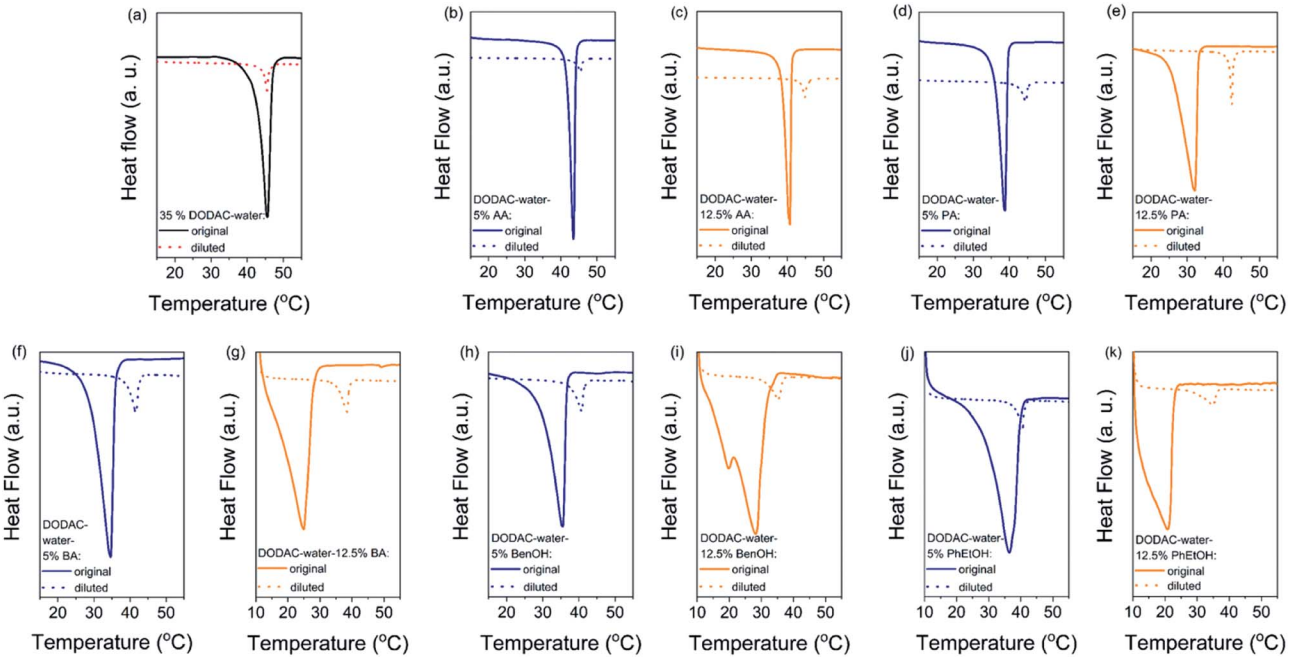

Fig. 1 (a) DSC heating thermograms of 35 wt% DODAC in water. Ternary surfactant mixtures with 5 wt% (blue color) and 12.5 wt% (orange color) of additive. Full line represents the original sample and dotted line corresponds to the sample diluted ten times. (b and c) Acetic acid (AA) samples. (d and e) Propionic acid (PA) samples. (f and g) Butyric acid (BA) samples. (h and i) Benzyl alcohol (BenOH) samples. (j and k) Phenoxyethanol (PhEtOH) samples. Endothermic down.

transition temperature *via* a similar mechanism and that they do not change the nature of the transition. However, the thermograms of the original samples of benzyl alcohol and phenoxyethanol, Fig. 1(h)–(k) full line, appear to be slightly different as they show a small plateau before the phase transition, which almost disappears with the larger amount (12.5 wt%) of additive in the mixture. At 12.5 wt%, the system contains a larger molar concentration of additive than of surfactant. At this high concentration of additive, the system containing benzyl alcohol results in a peak split, indicating the possible formation of an intermediate phase. The presence of these hydrotropes results in a significant decrease in the L_β–L_α transition temperature (to 21 °C). Fig. 2 summarizes the T_m values obtained for aqueous mixtures of DODAC in the presence of small and large amounts of the three SCFAs and the two hydrotrope molecules. These results show that the presence of the cosolutes in the surfactant system facilitates the transition from bilayers in the "solid" state to a "melted" state. A longer hydrophobic moiety of the cosolute results in a more significant decrease in the T_m.

The results from the diluted samples show that the addition of water to the surfactant system shifts the T_m back to higher temperatures as seen in Fig. 2. This indicates that these additives can be removed from the bilayers by water addition, thus restoring the gel phase. The enthalpy of the phase transition per mole of DODAC for the diluted samples was quite similar, although slightly lower when compared to the values of the "original" samples as summarized in Table 1. This effect can be attributed to a residual amount of cosolute remaining in the bilayers. However, the enthalpy of phase transition of the diluted mixtures with butyric acid is higher than the original sample. Butyric acid is the least polar molecule of the studied series of additives. Therefore, this additive may partially remain at the surfactant–water interface reducing the electrostatic repulsion between surfactant head-groups.

The presence of SCFAs and hydrotropes in the lamellar structure helped to tune the T_m. Upon dilution, the relative stability of the lamellar gel phase increases and hence the T_m was shifted to higher temperatures.

3.2. Surfactant packing in the diluted regime

Small and wide-angle X-ray scattering (SAXS/WAXS) was used to determine the chain packing and structure of the diluted surfactant–additive mixtures at temperatures below and above the gel-to-liquid crystalline (L_β–L_α) phase transition (T_m). The characteristic Bragg reflections with a peak ratio of 1 : 2 : 3… corresponding to lamellar structures were clearly observed in the small-angle regime. In addition, the wide-angle scattering profiles will give an indication on whether the alkyl chains of the bilayer are in a more solid-like or fluid-like state. For bilayers in the gel state (L_β), a sharp peak at around 1.5 $Å^{-1}$ is expected and this corresponds to the characteristic inter-acyl chain distance of 4.2 Å, whereas, for the fluid-like state (L_α), a shift to lower q values and a peak broadening is observed. Indeed the reflections in the wide-angle regime correspond to an inter-acyl chain distance of 4.1–4.2 Å for the L_β phase, and *ca.* 4.5–4.6 Å for the L_α phase.[23] The SAXS profiles of the original DODAC mixtures with short-chain fatty acids (SCFAs) and hydrotropes at temperatures below and above their T_m

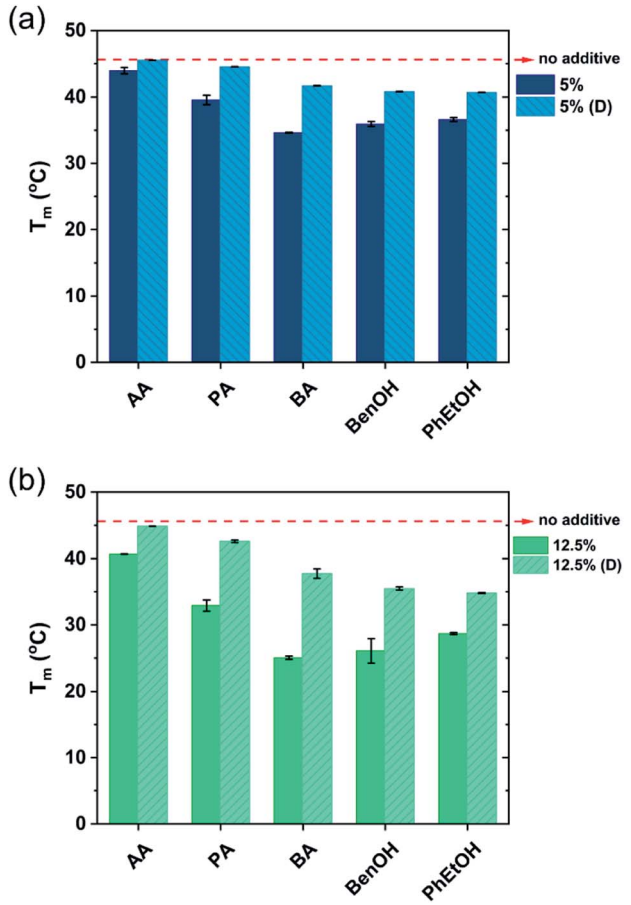

Fig. 2 Gel-to-liquid crystalline phase transition temperature (T_m) of the DODAC–water-additive mixtures. DODAC in the presence of: (a) 5 wt% of additive, before and after dilution ten times; (b) 12.5 wt% of additive, before and after dilution ten times. DODAC was fixed at 35 wt% for all the samples. AA-Acetic acid; PA-propionic acid; BA-butyric acid; BenOH-benzyl alcohol; PhEtOH-phenoxyethanol.

(ascertained by DSC)) were also recorded and the data confirms the lamellar structures, Fig. SI-1–SI-4 (ESI†). Additional features can be extracted from the SAXS and WAXS profiles, such as interlamellar *d*-spacing, polar layer thickness, non-polar layer thickness and the area per surfactant molecule as discussed in detail in our previous study.[14]

The surfactant mixtures were diluted ten times with water. These diluted mixtures display a rather thick water layer, and therefore they were characterized using synchrotron SAXS/WAXS beamline as the scattering is rather weak. The additive is expected to be at least partly removed from the water–DODAC interface. Indeed, after dilution the surfactant mixtures showed an increase in the T_m as discussed above. Thus, this suggests that the additives can be "washed away" from the mixed surfactant L_α phase, so that the DODAC gel phase is recovered. To verify this expected behavior, the alkyl chain packing was determined using WAXS data collected from synchrotron source, both below and above the transition temperature of these diluted mixtures.

The mixtures showed only one thermal transition under heating also after dilution of the sample (Fig. 1). As previously

Table 1 Values for the enthalpy of phase transition (ΔH_m) for DODAC–additive–water mixtures. The original mixtures correspond to 35.0 wt% of DODAC in the presence of 5.0 and 12.5 wt% of additive in water. Diluted samples were prepared by weighing a fraction of the original mixture and diluting in a 1 : 10 sample/water ratio. AA-Acetic acid; PA-propionic acid; BA-butyric acid; BenOH-benzyl alcohol; PhEtOH-phenoxyethanol

		ΔH_m (kJ mol^{-1})	
	Additive (wt%)	Original	Diluted
Acetic acid (AA)	5.0	44.2 ± 0.7	34.6 ± 1.3
	12.5	41.7 ± 1.9	39.8 ± 1.1
Propionic acid (PA)	5.0	37.0 ± 0.1	32.4 ± 2.1
	12.5	42.2 ± 1.3	34.3 ± 2.2
Butyric acid (BA)	5.0	30.8 ± 0.7	33.6 ± 1.3
	12.5	27.2 ± 1.4	28.7 ± 0.7
Benzyl alcohol (BenOH)	5.0	33.9 ± 1.6	34.3 ± 4.3
	12.5	—[a]	32.4 ± 0.7
Phenoxyethanol (PhEtOH)	5.0	34.3 ± 1.2	34.9 ± 0.4
	12.5	32.1 ± 5.6	37.0 ± 3.7

[a] Peak split that appears to indicate two thermal transitions, hence ΔH_m could not be determined.

reported, it can be assumed that lamellar surfactant systems display a large osmotic swelling which results in thick water layers in the lamellar structure.[23,24] Therefore, one may expect the same behavior for the DODAC–water–additive mixtures. Fig. 3 shows the SAXS and WAXS profiles of the diluted mixtures of DODAC in the presence 5 wt% of acetic acid at 20 and 55 °C. As identified in Fig. 3(a) and summarized in Table 2, the Bragg reflections follow an order of 1 : 2 : 3… which corresponds to a lamellar packing of the DODAC. At 20 °C, a sharp peak at 1.5285 Å^{-1}, which corresponds to the hydrocarbon chains in the gel phase with an inter-acyl chain distance of 4.1 Å, is observed (Fig. 3(b)). This confirms that the system features an L_β phase at 20 °C. The sharp Bragg peak in the WAXS data has disappeared at 55 °C and is replaced by a broad peak at lower *q* values, typically observed for bilayers in the fluid-like state. These results suggest that after dilution, the system does not lose its lamellar packing. This demonstrates the ability to tune the phase behavior of this surfactant system in the presence of additives by simple dilution. The original samples in the presence of additives display a lower T_m as compared to the sample in the absence of additives. The L_α phase in the presence of additives is thus relatively more stable for neat DODAC. The additive can be partially removed from the bilayers leading to a recovery of the L_β phase and consequently increase the T_m simply by dilution of the mixture with water. The same trend was found for all the diluted mixtures in the presence of 5 and 12.5 wt% of propionic and butyric acid, benzyl alcohol and phenoxyethanol, Fig. SI-5–SI-9 (ESI†).

3.3. Adsorbed amount and layer thickness upon rinsing

3.3.1. General aspects. The potential to tune the phase behavior by water addition lead us to explore the ability of these surfactant systems to be deposited onto surfaces. Silica was

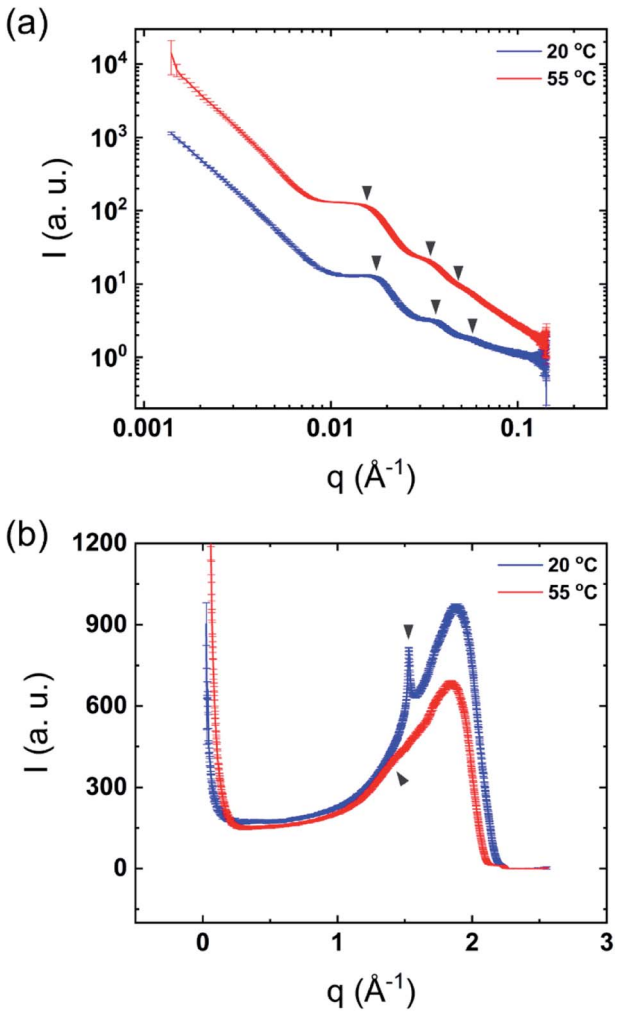

Fig. 3 Synchrotron scattering profiles of diluted mixtures of 5 wt% acetic acid in DODAC–water at 20 °C (below T_m) and 55 °C (above T_m). (a) SAXS and (b) WAXS.

Table 2 Values of the molecular distances of diluted mixtures of 5 wt% acetic acid in DODAC–water at 20 °C and 55 °C

		Temperature	
		20 °C	55 °C
SAXS	d_{100} (Å)	359	403
	d_{200} (Å)	176	201
	d_{300} (Å)	117	134
WAXS	Chain-to-chain (Å)	4.1	4.4
Phase		L_β	L_α

chosen as substrate to examine the deposition profile from the surfactant mixtures as a mimic of a negatively charged surface common in many applications. Previously it was demonstrated that deposition from surfactant/additive mixtures onto hydrophilic and hydrophobic silica are rather independent of the surface properties. Instead, deposition was found to be largely controlled by the solvency conditions rather than the attraction to the surface.[8] Here we used *in situ* null ellipsometry to provide us with information on the equilibrium and kinetic aspects of the adsorption process, both in terms of the surfactant adsorbed amount, Γ, and average thickness of the adsorbed film, d. In addition, the area occupied per surfactant molecule, a, can be derived from the adsorbed amount. This study focuses on the surface deposition when DODAC mixtures with a small amount of additive (5 wt%) and large amount of additive (12.5 wt%) were diluted.

In situ, time-resolved adsorption measurements were conducted using aqueous dispersions of DODAC in the presence of three short-chain fatty acids (SCFAs): acetic acid, propionic acid, butyric acid; and two hydrotrope molecules: benzyl alcohol and phenoxyethanol. The average thickness and adsorbed amount are presented in Fig. 4 and 5. The adsorption/deposition process was performed in a two-cycle fashion, start/stop rinsing and repeat of rinsing, as illustrated in Scheme 2.

Before discussing the details of the results for the different conditions (presented below in Fig. 4–7) we make some general observations. One striking aspect is that throughout the deposition process of a surfactant layer on the substrate, the variation of both the adsorbed amount and the thickness of the adsorbed layers is rather limited in spite of large differences in the composition of the bulk surfactant phase. Once deposited, the values remain stable and do not vary over long times and do not change on dilution. This rather well defined behavior is striking in view of the non-equilibrium conditions of the experiments.

A stable plateau obtained for the values of Γ and d occur after *ca.* 1000 s, with the exception of the sample with 12.5 wt% of propionic acid, Fig. 5(c). The time required to reach steady-state conditions depends on factors such as turbidity of the sample, the bulk concentration, *etc.*[18] Since ellipsometry is an optical technique, it requires a certain transparency of the medium. The turbid nature of the surfactant mixtures used here does not allow enough light to pass through the solution to follow the adsorption process. Nevertheless, seconds after the rinsing

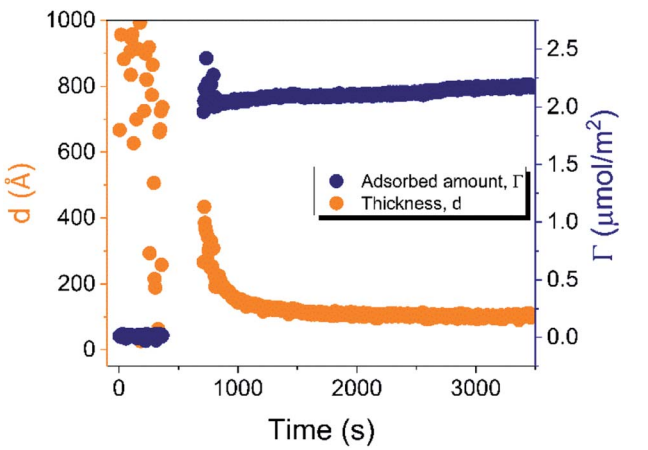

Fig. 4 Time evolution of the adsorbed amount (Γ) and average layer thickness (d) of DODAC–water mixture at the silica/water interface (T = 25 °C).

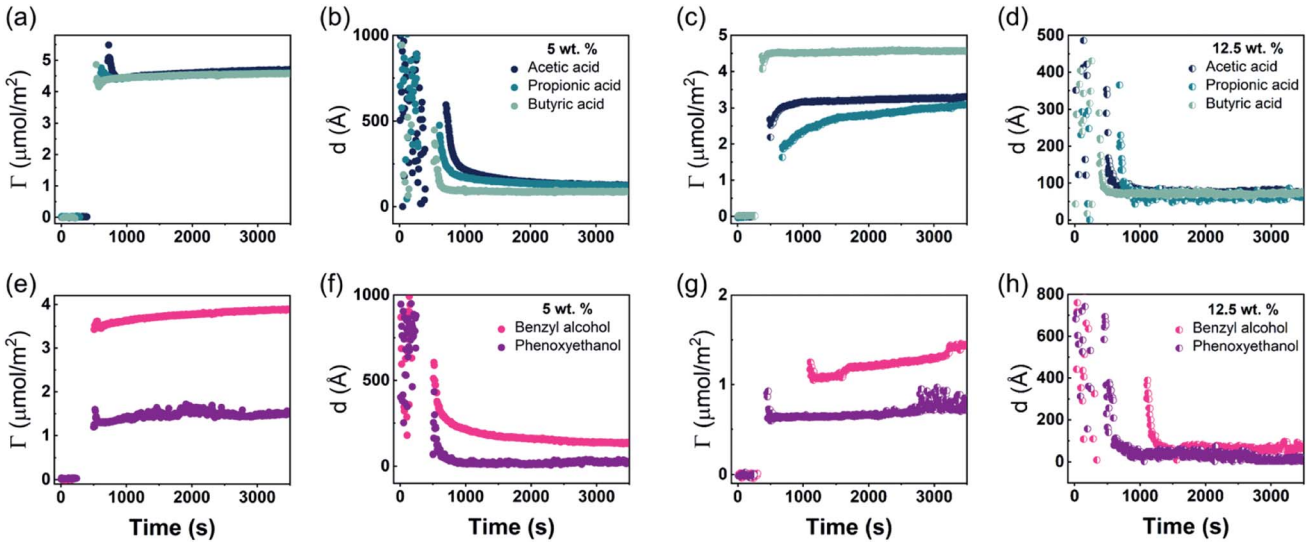

Fig. 5 Time evolution of the adsorbed amount, Γ, and average layer thickness, d, of DODAC–water–additive mixtures at the silica/water interface ($T = 25$ °C). (a), (b), (e) and (f) DODAC–water–5 wt% additive. (c), (d), (g) and (h) DODAC–water–12.5 wt% additive.

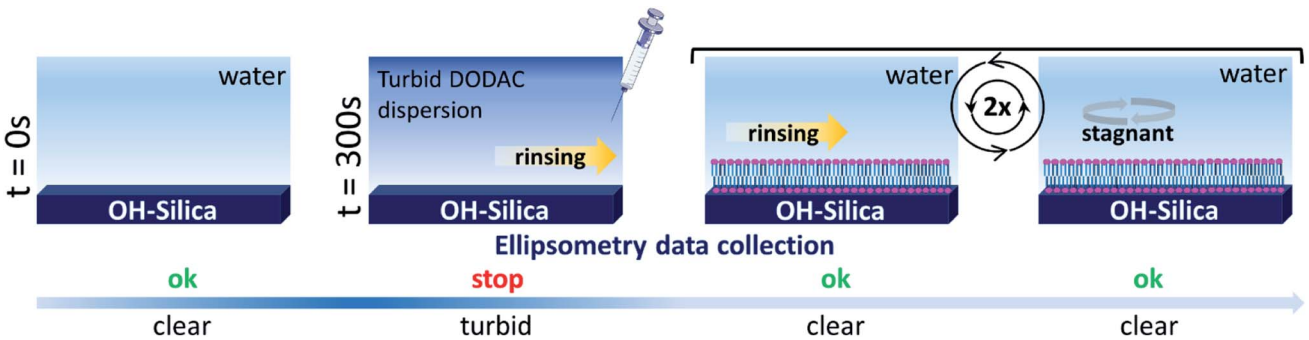

Scheme 2 Schematic representation of the experimental procedure used to study the deposition from DODAC–water–additive mixtures at the silica/water interface at 25 °C by *in situ* null ellipsometry. At $t = 0$ s the silica wafer was immersed in water. The diluted surfactant sample was injected into the cuvette at $t = 300$ s, followed by start/stop rinsing and repeat of rinsing.

process started, the instrument resumed the data collection. Therefore, there is a gap in the data between the moment that the sample was injected ($t = 300$ s) and a few seconds after the rinsing started ($t = 700$ s). Once the solution was sufficiently clear, the amount of surfactant adsorbed was determined to be 2.13 μmol m^{-2}, and the average layer thickness 107 Å. From the adsorbed amount, the area per surfactant molecule was determined to be 78 $Å^2$. This result is consistent with the area per surfactant molecule of bulk DODAC–water mixtures determined using SAXS in our previous study.[14]

Table 3 summarizes the properties of the adsorbed layers from the diluted DODAC–water–additive mixtures. Since all the films onto the hydrophilic silica are deposited from a highly diluted medium they are expected to be in the gel phase at 25 °C as demonstrated by the DSC and WAXS results. After the deposition on the surface, two cycles of rinsing were conducted, with no desorption being observed. The driving force for the formation of the surfactant film is mainly due to the inherent insolubility of DODAC in water but there is also an electrostatic attraction of the cationic surfactant to the negatively charged surface. The composition of the formed surfactant layer cannot be determined using ellipsometry, hence we can only evaluate the data in terms of the total amount deposited and the thickness of the formed layer. In the corresponding bulk sample, the DODAC bilayer was determined to be 28 Å-thick (using X-rays). This bilayer is rather thin when compared to the expected total thickness of two monolayers formed by an 18 carbon-chain oriented perpendicular to the interface. Such a small thickness value can be explained by the formation of a tilted and interdigitated DODAC bilayer in the gel phase.[14]

3.3.2. Deposition with added short-chain fatty acids. As mentioned above the phase transition between the gel and liquid crystalline phases can be tuned by the addition of certain solutes.[14,25–27] Here we investigate the effect of addition of three short-chain fatty acids (SCFAs), namely, acetic, propionic and butyric acid, which decrease the transition temperature markedly, on the amount of DODAC adsorbed on silica and the thickness of the deposited layer. The more hydrophobic SCFA

Table 3 Values of the adsorbed amount, Γ, average layer thickness, d, area per surfactant molecule, a, and pH of the diluted DODAC–water–additive mixtures

	Diluted sample	Adsorbed amount, Γ (μmol m^{-2})	Average thickness, d (Å)	Area per molecule, a (Å^2)	pH
	No additive	2.13 ± 0.04	107 ± 7	78	6.16
Small amount	5% acetic acid	4.71 ± 0.05	124 ± 7	35	2.99
	5% propionic acid	4.54 ± 0.04	136 ± 13	37	3.10
	5% butyric acid	4.53 ± 0.04	89 ± 2	37	3.14
	5% benzyl alcohol	3.84 ± 0.04	144 ± 8	43	4.43
	5% phenoxyethanol	1.48[a] ± 0.03	26 ± 5	112	7.22
Large amount	12.5% acetic acid	3.22 ± 0.03	76 ± 3	52	2.77
	12.5% propionic acid	2.91 ± 0.19	63 ± 2	57	2.84
	12.5% butyric acid	4.55 ± 0.02	72 ± 3	36	2.82
	12.5% benzyl alcohol	1.81[b] ± 0.01	62 ± 7	92	3.89
	12.5% phenoxyethanol	0.73 ± 0.06	38 ± 10	—	6.76

[a] Large scattering observed. [b] Result from the plateau in the steady-state.

will give rise to a less turbid dispersion. This was also supported by the DSC data that demonstrated that butyric acid contributed to a more stable DODAC L_α phase. This is shown in Fig. 5(a) and (b). The ellipsometer first resumed the data collection for butyric acid, followed by propionic acid, and lastly in system containing acetic acid. However, in high concentration of SCFA, the turbidity of the mixtures increased in the order butyric < acetic < propionic acid, hence a different behavior was observed. Therefore, the opaque DODAC dispersion in excess of propionic acid took longer time to reach a steady-state value. These results point to a stronger affinity of propionic acid to DODAC when in excess in the system. Consequently, a longer time is needed to remove the propionic acid from the DODAC bilayer during the rinsing process.

The mixtures with a small amount of short-chain fatty acid gave a larger adsorbed amount than the corresponding mixtures with an excess of short-chain fatty acid, except for the mixture with an excess of butyric acid. The same trend was found for the average film thickness. In line with previous results for polyelectrolyte–surfactant mixtures deposition increases when rinsing starts closer to the phase border.[9] On rinsing, a residual amount of SCFAs remains in the bilayers, which reduced the electrostatic repulsion between DODAC molecules, thus resulting in larger adsorbed amounts, and consequently, a smaller area per surfactant molecule.

3.3.3. Hydrotropes. The presence of hydrotrope molecules, benzyl alcohol and phenoxyethanol, results in smaller adsorbed amounts of DODAC, with the exception of benzyl alcohol at low concentration. Small amount (5 wt%) of benzyl alcohol in the mixture boosts the adsorbed amount by producing a closely packed DODAC bilayer with an area per surfactant molecule of 43 Å^2. On the contrary, a small amount of phenoxyethanol and high concentrations of both hydrotrope molecules result in lesser adsorbed amounts (<1.81 μmol m^{-2}) corresponding to larger areas per surfactant molecule (>92 Å^2), Fig. 5(e), (g) and Table 3. Ellipsometry measures the mean optical thickness, thus a thin layer or low adsorbed amount does not rule out that inhomogeneities with dense patches of adsorbed surfactant bilayers partially cover the substrate area. This phenomenon was observed in other surfactant systems studied at fluid interfaces that resulted in fluctuating ellipsometry signal from mobile patches of surfactant complex formed at the interfacial layer.[28]

The mixture with high concentration of benzyl alcohol was rather opaque, therefore it took a long time to resume ellipsometry data collection after the rinsing process had started, Fig. 5(g). Furthermore, three steady-state plateaus are identified during successive rinsing cycles, which feature an increase of the adsorbed amount with each rinsing step. This suggests that as benzyl alcohol is removed gradually, more DODAC deposited at each step. For all the other mixtures, the additive was "washed away" immediately during the first rinsing cycle. This evidence highlights the DODAC solvency effect as the driving force for surfactant adsorption onto silica.

For all the investigated additives, robust layers with a thickness of at least twice the length of the surfactant molecules are seen to be irreversibly deposited on hydrophilic silica.

3.3.4. Concentration effect. To understand the effects of the concentration of the mixture on the adsorbed DODAC amount and the thickness of the film formed, four different mixtures in the presence of excess butyric acid were studied. From the same diluted sample with butyric acid, increasing volumes (0.3, 0.5, 0.6 and 1.0 mL) were collected and added to the ellipsometry cuvette, and the volume was adjusted with water to a final volume of 5.0 mL. The added volume of the DODAC mixtures corresponds to concentrations of 3.6 mM (C1), 6.0 mM (C2), 7.2 mM (C3) and 12.0 mM (C4). The results of the adsorbed amount and layer thickness are presented in Fig. 6 and summarized in Table SI-1.†

The turbidity of the mixtures increased with concentration in the order C1 < C2 < C3 < C4, which is noticeable in Fig. 6. After the rinsing process started, only 158 seconds were needed to resume the data collection for the C1 mixture, whereas extra time was needed for the mixtures with high concentrations. The C4 mixture profile shows a considerably higher level of scattering when compared to the lower concentration samples, and

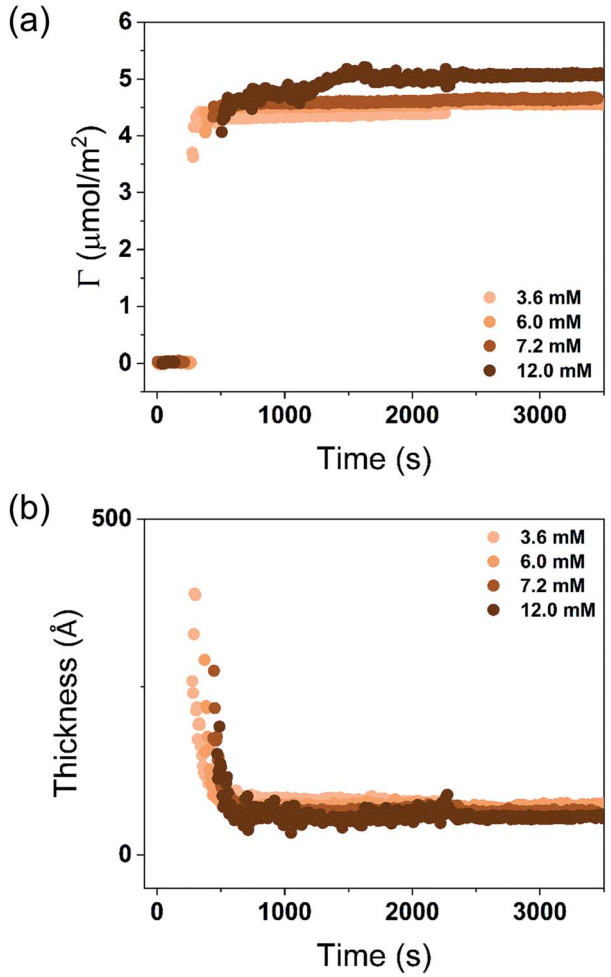

Fig. 6 (a) Time evolution of the adsorbed amount, Γ, and (b) average layer thickness, d, of DODAC–water–butyric acid mixtures at the silica/water interface (T = 25 °C). Mixtures with increasing concentration in the ellipsometry cuvette, 3.6 mM (C1), 6.0 mM (C2), 7.2 mM (C3) and 12.0 mM (C4).

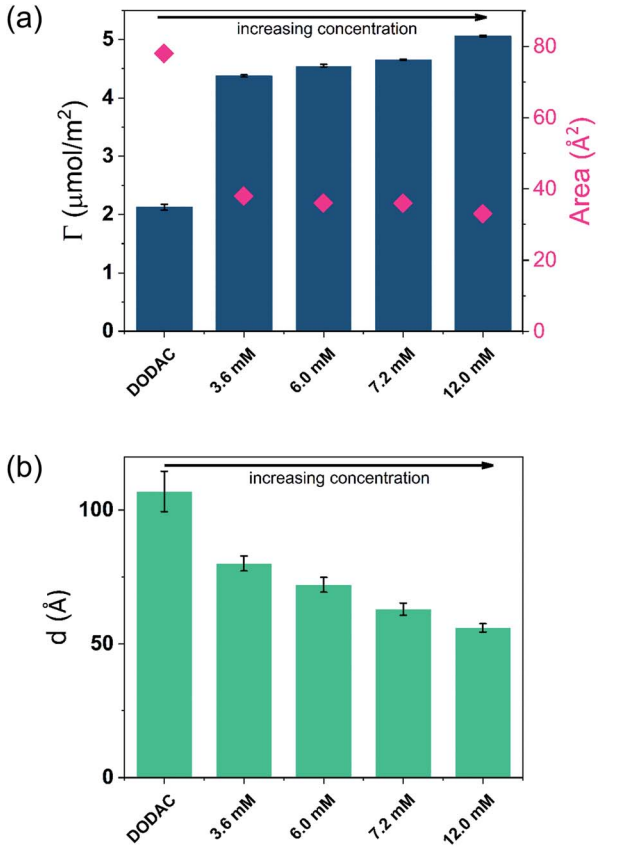

Fig. 7 (a) Adsorbed amount and area per surfactant molecule, and (b) average layer thickness of mixtures of 12.5 wt% of butyric acid in DODAC–water. Mixtures with increasing concentration in the ellipsometry cuvette, 3.6 mM (C1), 6.0 mM (C2), 7.2 mM (C3) and 12.0 mM (C4).

stabilized at a steady-state plateau only around 2400 s. This suggests that a more homogeneous layer of surfactant at low concentration was formed.

Though the adsorbed amount is higher and the adsorbed layer thinner in the presence of butyric acid than for the surfactant alone there is only a moderate variation of the deposition data with the concentration, Fig. 7. There is a slight increase of the adsorbed amount with the concentration. The origin of this effect is not clear but as discussed previously, the presence of SCFAs contributes to shield the electrostatic repulsion between DODAC head groups, which might enhance the amount of surfactant adsorbed on the substrate. As a result, the area per surfactant molecule was determined to decrease when compared to the mixture in the absence of SCFAs. The mixture C4 resulted in a slightly larger adsorbed amount of DODAC and smaller area per molecule, and the deposited layer from this mixture took longer time to reach steady-state values. It is noteworthy that the adsorbed amounts from mixtures with increasing concentration appear to be the same. More importantly, from the first and second columns in Fig. 7(a), the results suggest that butyric acid facilitates the deposition of robust and homogeneous layers of DODAC onto hydrophilic silica, even for the lowest concentration studied. The deposited layer of DODAC in the presence of butyric acid (from 56 to 89 Å) was slightly thinner compared to the deposited layer in the absence of additive (107 Å).

In the previous section, we have shown that thicker layers of DODAC were deposited when the additive was present in small amount (5 wt%), and the larger amount of additive (12.5 wt%) lead to a deposition of thinner layers of surfactant. The mixtures C1, C2, C3 and C4 are in the presence of larger concentration of butyric acid giving slightly thinner deposited layers of surfactant. Whereas there are some differences, a main finding is that well-defined layers are deposited and have a thickness slightly above the double length of the surfactant molecule.

4. Conclusion

The double-chain cationic surfactant, DODAC, has very low solubility in water but a large tendency to form stacked bilayer (lamellar) structures swelling with water. At low temperatures,

a gel phase, L_β, is formed with the surfactant molecules in a solid-like state whereas above a well-defined transition temperature, T_m, a liquid crystalline phase, L_α, is formed. As described in this work, a number of low molecular weight water-soluble compounds can lower the transition temperature substantially. Interestingly, on diluting samples of surfactant, additive and water, there is a spontaneous transition from the L_α to the L_β phase, ascribed to the dissociation of additive from the bilayers. Surfactants of the type studied have important applications for surface modification, like in hair conditioning. This is based on covering the substrate with the L_β phase. One problem in applications is to form stable formulations of the surfactant, the formulation typically consisting of kinetically stable dispersed particles of the L_β phase. The L_α phase, on the other hand, is thermodynamically stable over wide ranges and easier to formulate. One purpose of the present work was to investigate if stable samples of the L_α phase can spontaneously be changed into the L_β phase and subsequently deposited on a substrate. This was achieved *via* lowering the T_m using a water-soluble additive. On dilution, it is washed away, and the composition of the surfactant bilayer changed so that T_m is raised and a gel structure is formed. The WAXS results show that a sharp crystalline peak appears on dilution and that the chain-to-chain distance decreases, thus demonstrating the formation of a gel phase. Ellipsometry studies demonstrate that dilution of the surfactant–additive–water phases lead to the deposition of well-defined robust layers on a substrate. The adsorbed surfactant layers have a thickness of the order of the double surfactant molecule length and are stable and not affected by extensive dilution.

Conflicts of interest

There are no conflicts to declare.

Acknowledgements

The authors acknowledge useful discussions on SAXS and WAXS data fitting with Dr Pio Buenconsejo and financial support from Agency for Science, Technology and Research (A*STAR), Singapore (APG2013/016). Part of this research was undertaken on the SAXS and WAXS beamline (ID: M14264) at the Australian Synchrotron, part of ANSTO, and also at the Facility for Analysis, Characterisation, Testing and Simulation (FACTS) in Nanyang Technological University, Singapore.

References

1 R. G. Nuzzo and D. L. Allara, *J. Am. Chem. Soc.*, 1983, **105**, 4481–4483.
2 E. B. Troughton, C. D. Bain, G. M. Whitesides, R. G. Nuzzo, D. L. Allara and M. D. Porter, *Langmuir*, 1988, **4**, 365–385.
3 C. D. Bain, E. B. Troughton, Y. T. Tao, J. Evall, G. M. Whitesides and R. G. Nuzzo, *J. Am. Chem. Soc.*, 1989, **111**, 321–335.
4 I. R. Peterson, *J. Phys. D: Appl. Phys.*, 1990, **23**, 379–395.
5 B. Lindman, B. Medronho, L. Alves, C. Costa, H. Edlund and M. Norgren, *Phys. Chem. Chem. Phys.*, 2017, **19**, 23704–23718.
6 T. Nylander, Y. Samoshina and B. Lindman, *Adv. Colloid Interface Sci.*, 2006, **123**, 105–123.
7 E. Terada, Y. Samoshina, T. Nylander and B. Lindman, *Langmuir*, 2004, **20**, 1753–1762.
8 E. Terada, Y. Samoshina, T. Nylander and B. Lindman, *Langmuir*, 2004, **20**, 6692–6701.
9 A. V. Svensson, L. Huang, E. S. Johnson, T. Nylander and L. Piculell, *ACS Appl. Mater. Interfaces*, 2009, **1**, 2431–2442.
10 O. Santos, E. S. Johnson, T. Nylander, R. K. Panandiker, M. R. Sivik and L. Piculell, *Langmuir*, 2010, **26**, 9357–9367.
11 A. V. Svensson, E. S. Johnson, T. Nylander and L. Piculell, *ACS Appl. Mater. Interfaces*, 2010, **2**, 143–156.
12 M. Clauzel, E. S. Johnson, T. Nylander, R. K. Panandiker, M. R. Sivik and L. Piculell, *ACS Appl. Mater. Interfaces*, 2011, **3**, 2451–2462.
13 M. Kodama, M. Kuwabara and S. Seki, *Thermochim. Acta*, 1981, **50**, 81–91.
14 R. A. Gonçalves, B. Lindman, M. G. Miguel, T. Iwata and Y. M. Lam, *J. Colloid Interface Sci.*, 2018, **528**, 400–409.
15 S. Bjorklund, J. M. Andersson, Q. D. Pham, A. Nowacka, D. Topgaard and E. Sparr, *Soft Matter*, 2014, **10**, 4535–4546.
16 E. Sparr and H. Wennerstrom, *Curr. Opin. Colloid Interface Sci.*, 2011, **16**, 561–567.
17 J. Guo, J. C. S. Ho, H. Chin, A. E. Mark, C. Zhou, S. Kjelleberg, B. Liedberg, A. N. Parikh, N.-J. Cho, J. Hinks, Y. Mu and T. Seviour, *Phys. Chem. Chem. Phys.*, 2019, **21**, 11903–11915.
18 F. Tiberg and M. Landgren, *Langmuir*, 1993, **9**, 927–932.
19 R. M. A. Azzam and N. M. Bashara, *Ellipsometry and polarized light*, North-Holland Pub. Co., Amsterdam, New York, 1977, sole distributors for the U.S.A. and Canada, Elsevier North-Holland, 1977.
20 J. A. De Feijter, J. Benjamins and F. A. Veer, *Biopolymers*, 1978, **17**, 1759–1772.
21 A. Theisen, *Refractive Increment Data-book for Polymer and Biomolecular Scientists*, Nottingham University Press, 2000.
22 T. Tumolo, L. Angnes and M. S. Baptista, *Anal. Biochem.*, 2004, **333**, 273–279.
23 D. F. Evans and H. Wennerström, *The colloidal domain : where physics, chemistry, biology, and technology meet*, Wiley-VCH, New York, 2nd edn, 1999.
24 E. F. Marques and B. F. B. Silva, in *Encyclopedia of Colloid and Interface Science*, ed. T. Tadros, Springer Berlin Heidelberg, Berlin, Heidelberg, 2013, pp. 1202–1241, DOI: 10.1007/978-3-642-20665-8_169.
25 R. A. Demel and B. De Kruyff, *Biochim. Biophys. Acta, Rev. Biomembr.*, 1976, **457**, 109–132.
26 J. R. Usher, R. M. Epand and D. Papahadjopoulos, *Chem. Phys. Lipids*, 1978, **22**, 245–253.
27 R. N. McElhaney, *Chem. Phys. Lipids*, 1982, **30**, 229–259.
28 K. Tonigold, I. Varga, T. Nylander and R. A. Campbell, *Langmuir*, 2009, **25**, 4036–4046.

